

How Reproducible are Surface Areas Calculated from the BET Equation?

Johannes Osterrieth, James Rampersad, David Madden, Nakul Rampal, Luka Skoric, Bethany Connolly, Mark Allendorf, Vitalie Stavila, Jonathan Snider, Rob Ameloot, et al.

▶ **To cite this version:**

Johannes Osterrieth, James Rampersad, David Madden, Nakul Rampal, Luka Skoric, et al.. How Reproducible are Surface Areas Calculated from the BET Equation?. Advanced Materials, 2022, 34 (27), pp.2201502. 10.1002/adma.202201502 . hal-03677646v2

HAL Id: hal-03677646
https://hal.science/hal-03677646v2

Submitted on 7 Jul 2022

HAL is a multi-disciplinary open access archive for the deposit and dissemination of scientific research documents, whether they are published or not. The documents may come from teaching and research institutions in France or abroad, or from public or private research centers.

L'archive ouverte pluridisciplinaire **HAL**, est destinée au dépôt et à la diffusion de documents scientifiques de niveau recherche, publiés ou non, émanant des établissements d'enseignement et de recherche français ou étrangers, des laboratoires publics ou privés.

Check for updates

ADVANCED MATERIALS
www.advmat.de

How Reproducible are Surface Areas Calculated from the BET Equation?

*Johannes W. M. Osterrieth, James Rampersad, David Madden, Nakul Rampal, Luka Skoric, Bethany Connolly, Mark D. Allendorf, Vitalie Stavila, Jonathan L. Snider, Rob Ameloot, João Marreiros, Conchi Ania, Diana Azevedo, Enrique Vilarrasa-Garcia, Bianca F. Santos, Xian-He Bu, Ze Chang, Hana Bunzen, Neil R. Champness, Sarah L. Griffin, Banglin Chen, Rui-Biao Lin, Benoit Coasne, Seth Cohen, Jessica C. Moreton, Yamil J. Colón, Linjiang Chen, Rob Clowes, François-Xavier Coudert, Yong Cui, Bang Hou, Deanna M. D'Alessandro, Patrick W. Doheny, Mircea Dincă, Chenyue Sun, Christian Doonan, Michael Thomas Huxley, Jack D. Evans, Paolo Falcaro, Raffaele Ricco, Omar Farha, Karam B. Idrees, Timur Islamoglu, Pingyun Feng, Huajun Yang, Ross S. Forgan, Dominic Bara, Shuhei Furukawa, Eli Sanchez, Jorge Gascon, Selvedin Telalović, Sujit K. Ghosh, Soumya Mukherjee, Matthew R. Hill, Muhammed Munir Sadiq, Patricia Horcajada, Pablo Salcedo-Abraira, Katsumi Kaneko, Radovan Kukobat, Jeff Kenvin, Seda Keskin, Susumu Kitagawa, Ken-ichi Otake, Ryan P. Lively, Stephen J. A. DeWitt, Phillip Llewellyn, Bettina V. Lotsch, Sebastian T. Emmerling, Alexander M. Pütz, Carlos Martí-Gastaldo, Natalia M. Padial, Javier García-Martínez, Noemi Linares, Daniel Maspoch, Jose A. Suárez del Pino, Peyman Moghadam, Rama Oktavian, Russel E. Morris, Paul S. Wheatley, Jorge Navarro, Camille Petit, David Danaci, Matthew J. Rosseinsky, Alexandros P. Katsoulidis, Martin Schröder, Xue Han, Sihai Yang, Christian Serre, Georges Mouchaham, David S. Sholl, Raghuram Thyagarajan, Daniel Siderius, Randall Q. Snurr, Rebecca B. Goncalves, Shane Telfer, Seok J. Lee, Valeska P. Ting, Jemma L. Rowlandson, Takashi Uemura, Tomoya Iiyuka, Monique A. van derVeen, Davide Rega, Veronique Van Speybroeck, Sven M. J. Rogge, Aran Lamaire, Krista S. Walton, Lukas W. Bingel, Stefan Wuttke, Jacopo Andreo, Omar Yaghi, Bing Zhang, Cafer T. Yavuz, Thien S. Nguyen, Felix Zamora, Carmen Montoro, Hongcai Zhou, Angelo Kirchon, and David Fairen-Jimenez**

Dedicated to the memory of Francisco Rodriguez-Reinoso and his unique work in adsorption and porous materials

The ORCID identification number(s) for the author(s) of this article can be found under https://doi.org/10.1002/adma.202201502.

© 2022 The Authors. Advanced Materials published by Wiley-VCH GmbH. This is an open access article under the terms of the Creative Commons Attribution License, which permits use, distribution and reproduction in any medium, provided the original work is properly cited.

DOI: 10.1002/adma.202201502

J. W. M. Osterrieth, J. Rampersad, D. Madden, N. Rampal, B. Connolly, D. Fairen-Jimenez
The Adsorption & Advanced Materials Laboratory (A²ML)
Department of Chemical Engineering & Biotechnology
University of Cambridge
Philippa Fawcett Drive, Cambridge CB3 0AS, UK
E-mail: df334@cam.ac.uk

L. Skoric
Cavendish Laboratory
University of Cambridge
JJ Thomson Avenue, Cambridge CB3 0HE, UK

M. D. Allendorf, V. Stavila, J. L. Snider
Sandia National Laboratories
7011 East Avenue, Livermore, CA 94550, USA

R. Ameloot, J. Marreiros
cMACS
Department of Microbial and Molecular Systems (M^2S)
KU Leuven
Leuven 3001, Belgium

C. Ania
CEMHTI
CNRS (UPR 3079)
Université d'Orléans
Orléans 45071, France

D. Azevedo, E. Vilarrasa-Garcia, B. F. Santos
LPACO2/GPSA
Department of Chemical Engineering
Federal University of Ceará
Fortaleza (CE) 60455-760, Brazil

X.-H. Bu, Z. Chang
School of Materials Science and Engineering
National Institute for Advanced Materials
Nankai University
Tianjin 300350, China

H. Bunzen
Chair of Solid State and Materials Chemistry
Institute of Physics
University of Augsburg
Universitaetsstrasse 1, 86159 Augsburg, Germany

N. R. Champness, S. L. Griffin
School of Chemistry
University of Nottingham
University Park, Nottingham NG7 2RD, UK

B. Chen, R.-B. Lin
Department of Chemistry
University of Texas at San Antonio
One UTSA Circle, San Antonio, TX 78249-0698, USA

B. Coasne
Univ. Grenoble Alpes
CNRS
LIPhy
Grenoble 38000, France

S. Cohen, J. C. Moreton
Department of Chemistry and Biochemistry
University of California
San Diego, La Jolla, CA 92093, USA

Y. J. Colón
Department of Chemical and Biomolecular Engineering
University of Notre Dame
Notre Dame, IN 46556, USA

L. Chen, R. Clowes
Leverhulme Research Centre for Functional Materials Design
Materials Innovation Factory and Department of Chemistry
University of Liverpool
Liverpool L7 3NY, UK

F.-X. Coudert
Chimie ParisTech
PSL University
CNRS
Institut de Recherche de Chimie Paris
Paris 75005, France

Y. Cui, B. Hou
School of Chemistry and Chemical Engineering
Shanghai Jiaotong University
800 Dongchuan Road, Minhang District, Shanghai 200240, China

D. M. D'Alessandro, P. W. Doheny
School of Chemistry
The University of Sydney
New South Wales 2006, Australia

M. Dincă, C. Sun
Department of Chemistry
Massachusetts Institute of Technology
Cambridge, MA 02139, USA

C. Doonan, M. T. Huxley
Centre for Advanced Nanomaterials and Department of Chemistry
The University of Adelaide
North Terrace, Adelaide SA 5000, Australia

J. D. Evans
Department of Inorganic Chemistry
Technische Universität Dresden
Bergstrasse 66, 01062 Dresden, Germany

P. Falcaro, R. Ricco
Institute of Physical and Theoretical Chemistry
Graz University of Technology
Graz 8010, Austria

O. Farha, K. B. Idrees, T. Islamoglu
Department of Chemistry and International Institute of Nanotechnology
Northwestern University
2145 Sheridan Road, Evanston, IL 60208, USA

P. Feng, H. Yang
Department of Chemistry
University of California
Riverside, CA 92521, USA

R. S. Forgan, D. Bara
WestCHEM, School of Chemistry
University of Glasgow
Glasgow G12 8QQ, UK

S. Furukawa, E. Sanchez
Institute for Integrated Cell-Material Sciences
Kyoto University
Yoshida, Sakyo-ku, Kyoto 606-8501, Japan

J. Gascon, S. Telalović
KAUST Catalysis Center (KCC)
King Abdullah University of Science and Technology
P.O. Box 4700, Thuwal-Jeddah 23955-6900, Kingdom of Saudi Arabia

S. K. Ghosh, S. Mukherjee
Department of Chemistry
Indian Institute of Science Education and Research (IISER) Pune
Dr. Homi Bhabha Road, Pashan, Pune 411008, India

M. R. Hill, M. M. Sadiq
CSIRO
Private Bag 33, Clayton South MDC, Clayton, VIC 3169, Australia

M. R. Hill, M. M. Sadiq
Department of Chemical Engineering
Monash University
Clayton, VIC 3168, Australia

P. Horcajada, P. Salcedo-Abraira
Advanced Porous Materials Unit (APMU)
IMDEA Energy
Avda. Ramón de la Sagra 3, (Móstoles) Madrid E-28935, Spain

K. Kaneko, R. Kukobat
Research Initiative for Supra-Materials
Shinshu University
Nagano 380-8553, Japan

J. Kenvin
Micromeritics Instrument Corporation
Norcross, GA 30093, USA

S. Keskin
Department of Chemical and Biological Engineering
Koc University
Rumelifeneri Yolu Sariyer, Istanbul 34450, Turkey

© 2022 The Authors. Advanced Materials published by Wiley-VCH GmbH

S. Kitagawa, K.-i. Otake
Institute for Integrated Cell-Material Sciences (WPI-iCeMS)
Kyoto University Institute for Advanced Study (KUIAS)
Kyoto University
Yoshida Ushinomiya-cho, Sakyo-ku, Kyoto 606-8501, Japan

R. P. Lively, S. J. A. DeWitt, D. S. Sholl, R. Thyagarajan, K. S. Walton, L. W. Bingel
School of Chemical & Biomolecular Engineering
Georgia Institute of Technology
Atlanta, GA 30332, USA

P. Llewellyn
CNRS / Aix-Marseille Univ./Total
Marseille 64018, France

B. V. Lotsch, S. T. Emmerling, A. M. Pütz
Max Planck Institute for Solid State Research
Heisenbergstrasse 1, 70569 Stuttgart, Germany

B. V. Lotsch, S. T. Emmerling, A. M. Pütz
Department of Chemistry
University of Munich (LMU)
Butenandtstrasse 5-13, 81377 Munich, Germany

C. Martí-Gastaldo, N. M. Padial
Instituto de Ciencia Molecular (ICMol)
Universitat de València
Paterna, València 46980, Spain

J. García-Martínez, N. Linares
Laboratorio de Nanotecnología Molecular
Departamento de Química Inorgánica
Universidad de Alicante
Ctra. San Vicente-Alicante s/n, San Vicente del Raspeig E-03690, Spain

D. Maspoch
ICREA
Pg. Lluís Companys 23, Barcelona 08010, Spain

D. Maspoch, J. A. Suárez del Pino
Catalan Institute of Nanoscience and Nanotechnology (ICN2)
CSIC and the Barcelona Institute of Science and Technology
Campus UAB, Bellaterra, Barcelona 08193, Spain

P. Moghadam, R. Oktavian
Department of Chemical and Biological Engineering
The University of Sheffield
Sheffield S10 2TN, UK

R. E. Morris, P. S. Wheatley
School of Chemistry
University of St Andrews
North Haugh, St Andrews KY16 9ST, UK

J. Navarro
Departamento de Química Inorgánica
Universidad de Granada
Granada 18071, Spain

C. Petit, D. Danaci
Barrer Centre
Department of Chemical Engineering
Imperial College London
London SW7 2AZ, UK

M. J. Rosseinsky, A. P. Katsoulidis
Materials Innovation Factory
Department of Chemistry
University of Liverpool
Liverpool L7 3NY, UK

M. Schröder, X. Han, S. Yang
School of Chemistry
The University of Manchester
Manchester M13 9PL, UK

C. Serre, G. Mouchaham
Institut des Matériaux Poreux de Paris
Ecole Normale Supérieure
ESPCI Paris
CNRS
PSL University
Paris 75005, France

D. Siderius
Chemical Sciences Division
National Institute of Standards and Technology
Gaithersburg, MD 20899-8320, USA

R. Q. Snurr
Department of Chemical & Biological Engineering
Northwestern University
2145 Sheridan Road, Evanston, IL 60208, USA

R. B. Goncalves
Department of Chemistry
Northwestern University
2145 Sheridan Road, Evanston, IL 60208, USA

S. Telfer, S. J. Lee
MacDiarmid Institute for Advanced Materials and Nanotechnology
Institute of Fundamental Sciences
Massey University
Palmerston North 4442, New Zealand

V. P. Ting, J. L. Rowlandson
Department of Mechanical Engineering
University of Bristol
Bristol BS8 1TR, UK

T. Uemura, T. Iiyuka
Department of Advanced Materials Science
Graduate School of Frontier Sciences
The University of Tokyo
5-1-5 Kashiwanoha, Kashiwa, Chiba 277-8561, Japan

M. A. van der Veen, D. Rega
Department of Chemical Engineering
Delft University of Technology
van der Maasweg 9, Delft 2629HZ, The Netherlands

V. Van Speybroeck, S. M. J. Rogge, A. Lamaire
Center for Molecular Modeling (CMM)
Ghent University
Technologiepark 46, Zwijnaarde B-9052, Belgium

S. Wuttke, J. Andreo
BCMaterials
Basque Center for Materials
Applications and Nanostructures
UPV/EHU Science Park, Leioa 48940, Spain

S. Wuttke, J. Andreo
IKERBASQUE
Basque Foundation for Science
Bilbao 48009, Spain

O. Yaghi, B. Zhang
Department of Chemistry
University of California – Berkeley
Kavli Energy Nanoscience Institute at UC Berkeley
Berkeley, CA 94720, USA

O. Yaghi
Berkeley Global Science Institute
Berkeley, CA 94720, USA

C. T. Yavuz, T. S. Nguyen
Department of Chemical and Biomolecular Engineering
Korea Advanced Institute of Science and Technology (KAIST)
Yuseong-gu, Daejeon 34141, South Korea

F. Zamora, C. Montoro
Departamento de Química Inorgánica
Universidad Autónoma de Madrid
Madrid 28049, Spain

H. Zhou, A. Kirchon
Department of Chemistry
Texas A&M University
College Station, TX 77843, USA

© 2022 The Authors. Advanced Materials published by Wiley-VCH GmbH

Porosity and surface area analysis play a prominent role in modern materials science. At the heart of this sits the Brunauer–Emmett–Teller (BET) theory, which has been a remarkably successful contribution to the field of materials science. The BET method was developed in the 1930s for open surfaces but is now the most widely used metric for the estimation of surface areas of micro- and mesoporous materials. Despite its widespread use, the calculation of BET surface areas causes a spread in reported areas, resulting in reproducibility problems in both academia and industry. To prove this, for this analysis, 18 already-measured raw adsorption isotherms were provided to sixty-one labs, who were asked to calculate the corresponding BET areas. This round-robin exercise resulted in a wide range of values. Here, the reproducibility of BET area determination from identical isotherms is demonstrated to be a largely ignored issue, raising critical concerns over the reliability of reported BET areas. To solve this major issue, a new computational approach to accurately and systematically determine the BET area of nanoporous materials is developed. The software, called "BET surface identification" (BETSI), expands on the well-known Rouquerol criteria and makes an unambiguous BET area assignment possible.

1. Main

The Brunauer–Emmett–Teller (BET) equation is arguably one of the most used equations in physical chemistry and porosimetry. Since its conception in the 1930s[1] to estimate open surfaces whilst working with non-microporous adsorbents of the time such as Fe/Cu catalysts, silica gel, and charcoal, it found widespread use in the characterization of synthetic zeolites.[2] Furthermore, it has gained considerable momentum following the discovery of more complex porous materials such as mesoporous silicas,[3–5] porous coordination polymers (PCPs),[6] metal–organic frameworks (MOFs)[7] and covalent organic frameworks (COFs).[8] Novel porous materials are of significant academic and industrial interest due to their applications in gas storage and separation,[9–12] catalysis,[13] sensing,[14,15] and drug delivery.[16] To assess their adsorptive properties, Langmuir was the first to relate gas adsorption isotherms to surface areas, assuming only monolayer adsorption.[17] This was in contrast to Dubinin's proposition of micropore volumes for microporous materials.[18] Langmuir's adsorption theory was later extended to multilayer adsorption, resulting in the titular BET model. Even though the BET theory was not developed for describing adsorption in the microporosity, the BET area is now the de facto standard for the characterization of any porous material. Indeed, it has been recognized by the International Union of Pure and Applied Chemistry (IUPAC) as "the most widely used procedure for evaluating the surface area of porous and finely divided materials."[19,20] Furthermore, it has been an International Organization for Standardization (ISO) standard for surface area determination since 1995.[21] This makes it, arguably, the most important figure of merit for porous materials, including microporous ones. Looking at the literature, it is clear that the idea of monolayer coverage or even the concept of surface area are necessarily idealized and therefore could be inaccurate descriptions for microporous materials.[22] Indeed, IUPAC warns users to apply "extreme caution [when using the BET equation] in the presence of micropores. (...) [The BET area] represents an apparent surface area, which may be regarded as a useful adsorbent 'fingerprint'."[19] This more nuanced understanding of the BET area is mirrored in the writing of Rouquerol et al., "the meaning of the BET surface is (...) that it embraces the major part of the amount of adsorptive in energetic interaction with the surface."[22] Despite these cautionary words, the BET area remains a deeply engrained metric in the fields of physical chemistry and materials science. Given the broad use of the BET equation, it is not surprising to see that much has been written on the applicability and the accuracy of the BET theory—that is, its model of the adsorption process—and on the reproducibility of the raw data, i.e., the adsorption isotherm.[23–26]

Since the development of the first porous materials, there has been a sharp rise in the design of highly ordered and structured porous materials (Figure S1, Supporting Information).[27,28] The advent of materials with more complex pore networks and dynamic frameworks through material design strategies such as reticular chemistry has given rise to reported BET areas in excess of 8000 $m^2\ g^{-1}$.[10,29–34] Often, these modern materials have complex adsorption isotherms which are more problematic or ambiguous to fit to the BET model, e.g. several steps can occur due to different pore types and/or flexibility being present in the material.[35] In response, a new generation of porosimetry equipment with pressure transducers capable of recording high-resolution gas adsorption isotherms at ultralow pressures ($<10^{-5}$ mmHg) has been developed. However, reliance on manual calculations of surface areas using the BET method remains commonplace. In this context, "manual" refers to the judicious selection of a pressure range by a scientist, be it through a self-developed spreadsheet or commercial software. This raises the question of the reproducibility of BET calculations from the same isotherm. An adsorption isotherm with 150 points has more than 10 000 consecutive combinations of points, all of which are potentially correct fitting ranges and will return different BET areas. The answer to the question of which is the optimal fitting region is far from obvious, and the consequence of any irreproducibility or different interpretations are serious. Consider two groups synthesizing the same compound and reporting two different BET areas; Sample A is reported to have a BET area of 1500 $m^2\ g^{-1}$ and Sample B's reported BET area is 2000 $m^2\ g^{-1}$. Unless there is a common standard and protocol for calculating BET areas, we cannot say for certain that the quality and adsorption performance of Sample A is lower than that of Sample B. Indeed, the lack of reproducibility of MOF syntheses and adsorption performance, by comparing reported BET areas, has been highlighted already, but the natural spread of BET calculations was not included in the analysis.[36]

© 2022 The Authors. Advanced Materials published by Wiley-VCH GmbH

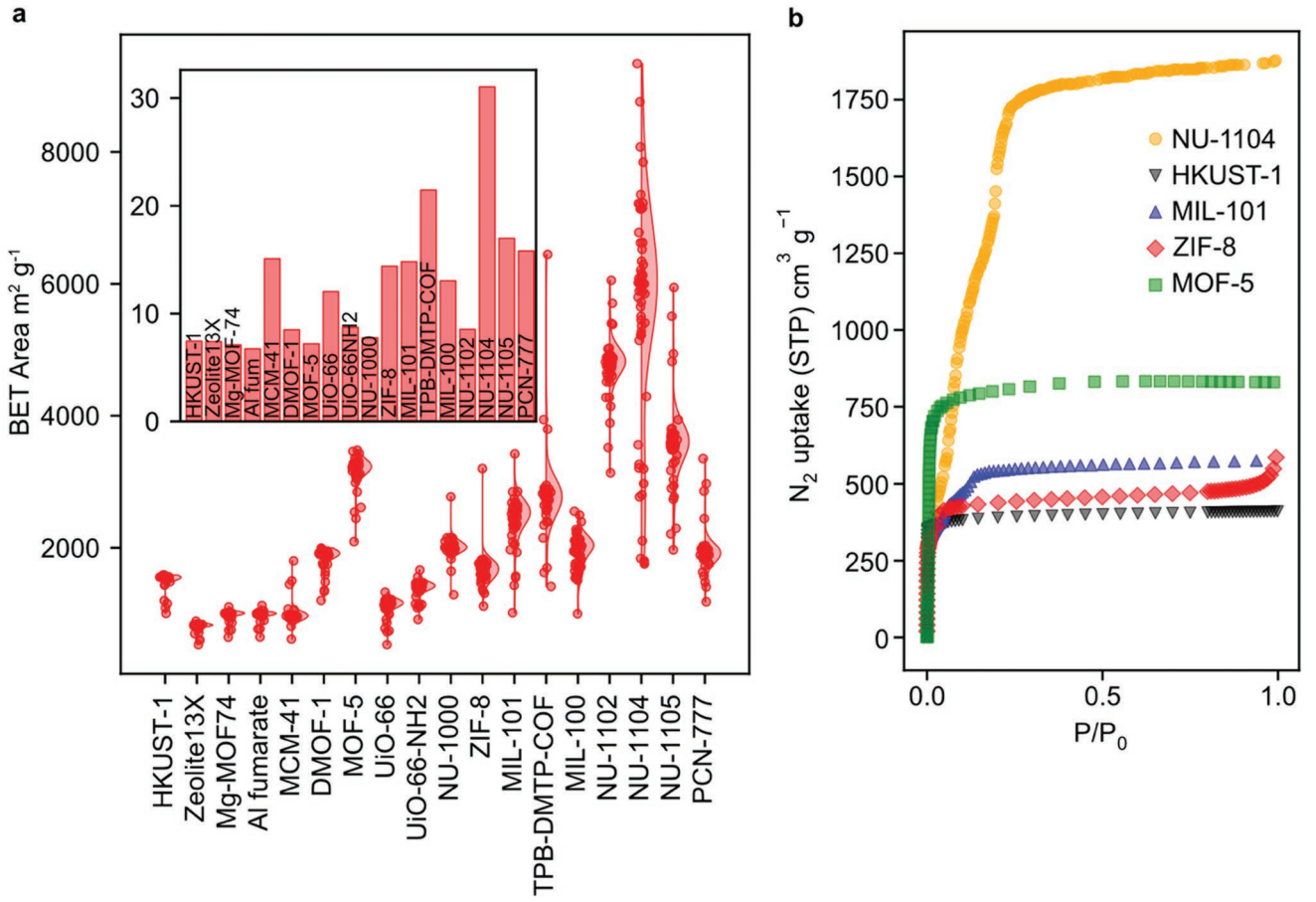


Figure 1. Round-robin results of BET area calculation. a) Distribution of BET areas from identical isotherms as calculated by 61 laboratories with an expertise in adsorption science and synthesis of porous materials. Superimposed are normalized probability distribution functions obtained by kernel density estimation (sample size for each material, $n = 61$). Inset shows the coefficient of variation (relative standard deviation) of results for each material. b) Exemplary isotherms for materials shown in (a). The large spread of BET areas reported for NU-1104 is due to the unusual shape of its adsorption isotherm, making manual BET fits difficult.

The eponymously named Rouquerol criteria (Section S2, Supporting Information) aim to ensure good practice in identifying a valid fitting range, and, as such, they have found widespread acceptance in the literature and have been adopted in both IUPAC and ISO standards.[19–22,24,25,37] Despite this safeguard, we herein propose that current BET area calculations are irreproducible for two reasons: first, the Rouquerol criteria are indeterminate in identifying the correct fitting region, as they apply to multiple regions simultaneously. Second, even if they were determinate, they are too cumbersome and lengthy to implement and are therefore often neglected in practice. This dilemma is reminiscent of the Skeptic's Argument from Gorgias, here paraphrased: i) the BET area does not exist (e.g., for microporous materials); ii) even if it exists, it cannot be systematically and unequivocally calculated (i.e., determined by the Rouquerol criteria).

To prove our hypothesis and to assess the current spread of BET calculation results, we have shared a dataset of 18 isotherms (reported as relative pressure versus amount adsorbed), already measured, and representing four classes of micro- and mesoporous materials (zeolites, mesoporous silicas, MOFs, and COFs) with 61 laboratories with expertise in adsorption science and synthesis of porous materials. In this round-robin exercise, we asked the researchers to calculate the BET areas in the way they saw most fit. More details about the specific materials and the adsorption isotherms, sampled both from our laboratory and from the NIST/ARPA-E database,[38] are included in the Supporting Information, (Section S1). To avoid any recognition bias, all isotherms were anonymized and scaled-off arbitrarily. **Figure 1**a shows the large spread of results obtained from manual calculations of BET areas in the round-robin experiment, the full details can be found anonymized in the Supporting Information: tabulated in Section S3, and represented graphically in Section S4. Most groups (90%) reported using the Rouquerol criteria in their manual calculation, 23% used a commercial software package, and 6% used a self-developed code. Details on the methods for each group can be found in Section S11 of the Supporting Information. Bar a few exceptions, virtually no two groups of experts reported identical BET areas for any given isotherm. We observed a spread of at least 300 $m^2\ g^{-1}$ for each isotherm; however, that number was significantly higher for some individual isotherms. For NU-1104, a modern MOF with substantial porosity (isotherm Figure 1b),[32] the highest estimate of 9341 $m^2\ g^{-1}$ and the lowest estimate of

© 2022 The Authors. Advanced Materials published by Wiley-VCH GmbH

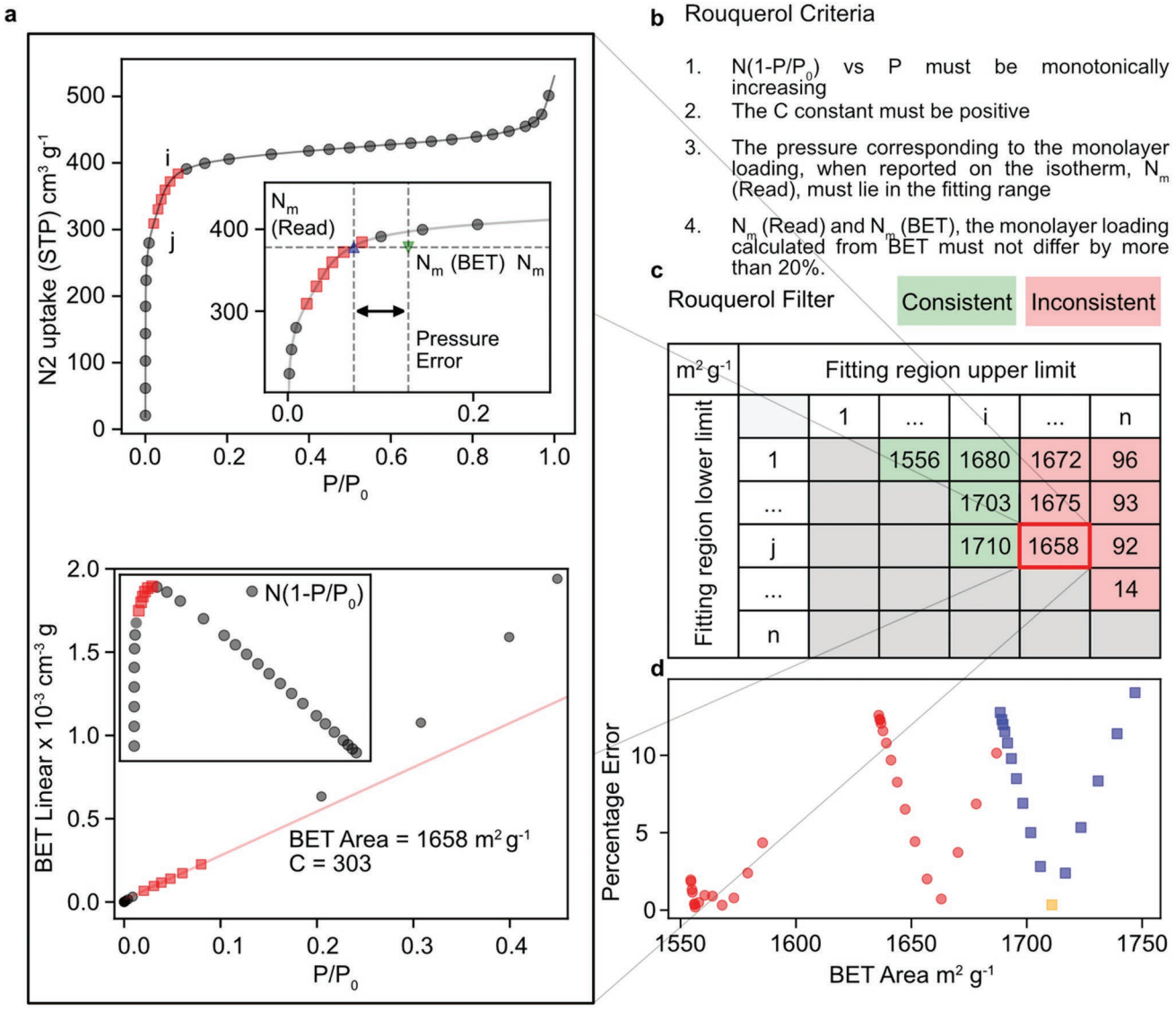


Figure 2. Working principle for the BETSI algorithm. a) The isotherm is shown with a particular fitting region highlighted in red. The linear BET equation is applied, and an ordinary least-squares regression is applied to the fitting region. b) Subsequent checks against the Rouquerol criteria[24] are performed (insets) and c) valid fits are passed. The analysis shown in (a) is repeated for all consecutive combinations of points on the isotherm. A results matrix with $n \times n$ dimensionality stores all acceptable and rejected fits. d) All acceptable BET areas are output and plotted against the percentage error under the 4th Rouquerol criterion ((a), top inset). All BET areas ending on the highest permissible point under the 1st Rouquerol criterion ((a), bottom inset, maximum in the $N(1 - (P/P_0))$ function) are labelled as the isotherm knee and shown in blue. The BETSI Optimal BET area (yellow) belongs to the isotherm knee group and has the lowest percentage error under the 4th Rouquerol criterion.

1757 $m^2\ g^{-1}$ differed by an astonishing 7584 $m^2\ g^{-1}$, making the highest estimate more than five times higher than the lowest estimate. The spread of values for frequently reproduced MOFs such as HKUST-1, MOF-5, and ZIF-8 was slightly smaller than that of literature cited values.[36] While this observation affirms the natural assumption that material synthesis and isotherm measurement play a more important role in determining the BET area than the calculation, we can nevertheless attribute a significant portion of this spread to current BET fittings. The results of this social study demonstrate that there is significant variation in BET area calculations from the same isotherm, as it is extremely unlikely for two researchers to select identical fitting regions. At this point, we propose a novel method that not only systematically selects an optimal fitting region but does so by eliminating all other hypothetical fitting regions. With thousands of consecutive combinations of points, the large number of potential fittings is impossible to carry out manually.

To solve the problem of manual BET fitting, we developed a computational tool for BET analysis, BET surface identification (BETSI). This tool makes an unambiguous calculation of the BET area based on the original Rouquerol criteria but modified to prevent manual interaction, requiring only the adsorption isotherm as input data. As such, the results obtained from the round-robin evaluation were compared with the BETSI calculations to assess the inter-rater reliability of manual BET calculations. **Figure 2** shows the working principle of the BETSI

© 2022 The Authors. Advanced Materials published by Wiley-VCH GmbH

Table 1. Results of BETSI analysis and round-robin evaluation for the isotherms used in the study. Material, isotherm of material under investigation; BETSI, optimal BET area predicted by BETSI; BETSI range, full spread of BET areas that pass under BETSI; BETSI variation coefficient, relative standard deviation of BET areas that pass under BETSI; pass rate, number of BET areas that pass under BETSI expressed as a fraction of all hypothetical fittings; round-robin average, mean of BET areas calculated in round-robin evaluation (sample size for each material, $n = 61$); round-robin range, full spread of BET areas determined in round-robin evaluation; round-robin variation coefficient, relative standard deviation of BET areas calculated in round-robin evaluation; hit rate, fraction of BET areas calculated in the round-robin evaluation that lie within the BETSI range.

Material	BETSI [$m^2\ g^{-1}$]	BETSI range [$m^2\ g^{-1}$]	BETSI variation coefficient [%]	Pass rate [%]	Round-robin average [$m^2\ g^{-1}$]	Round-robin range [$m^2\ g^{-1}$]	Round-robin variation coefficient [%]	Hit rate [%]
HKUST-1	1556	8	0.090	2.419	1520	583	7.451	52
Zeolite13X	833	4	0.140	0.538	813	356	7.405	35
Mg-MOF74	1010	5	0.114	2.300	990	459	7.101	48
Al-Fumarate	1007	14	0.398	1.736	989	478	6.740	60
MCM-41	1001	60	1.573	3.329	994	1186	15.090	85
DMOF-1	1924	4	0.074	0.107	1860	795	8.500	15
MOF-5	3255	20	0.250	0.071	3170	1382	7.203	13
UiO-66	1145	91	1.901	0.870	1120	796	12.045	65
UiO-66-NH_2	1424	285	4.710	1.722	1388	750	8.727	48
NU-1000	2068	160	1.619	4.218	2014	1486	7.752	80
ZIF-8	1709	188	3.718	0.861	1672	2085	14.396	58
MIL-101	2446	680	8.353	3.738	2429	2404	14.816	78
TPB-DMTP-COF	2875	711	7.298	5.375	2787	5031	21.472	80
MIL-100	2199	616	7.611	12.111	1964	1554	13.042	78
NU-1102	4931	204	1.139	0.862	4770	2915	8.541	38
NU-1104	5684	235	1.327	0.024	5553	7584	31.047	5
NU-1105	3635	0	0.000	0.011	3585	3974	16.991	0
PCN-777	2079	483	5.624	6.960	1946	2168	15.814	87

algorithm on a simplified N_2 adsorption isotherm at 77 K for ZIF-8 (full details can be found in the Supporting Information, Section S5). First, the linearized BET equation is fitted to a particular region of the isotherm using an ordinary least-squares (OLS) regression (Figure 2a). The top panel shows the isotherm with a fitting region highlighted in red, and the OLS regression is shown below. The plot insets show the checks against the Rouquerol criteria (Figure 2b). If all criteria are met, the fitting is passed. This calculation is looped over all data intervals of at least 10 points on the isotherm. The resulting BET fits are stored in a large $n \times n$ matrix, where the (j,i)-matrix element corresponds to a fitting region starting at the jth-point and ending on the ith-point (Figure 2c). All valid fitting results are output and plotted against the percentage error under the 4th Rouquerol criterion (Figure 2d). Alongside, BETSI outputs all other BET parameters, such as monolayer capacity and the C constant, as well as full regression diagnostics (Section S5, Supporting Information).

Since multiple fittings comply with the Rouquerol criteria (Figure 2c,d), BETSI demonstrates that an unambiguous assignment of the BET area is impossible under the Rouquerol criteria alone. This proves our hypothesis that the criteria in their current form are indeterminate. For the prototypical ZIF-8 isotherm, a flexible MOF with narrow windows,[35] valid BET areas fall within a range of 1550 and 1750 $m^2\ g^{-1}$ (Figure 2c,d). BETSI assigns special relevance to fitting ranges that end on the highest permissible point, which are usually dictated by the 1st Rouquerol criterion, and labels these as the isotherm knee. Beyond the isotherm knee, adsorptive activity decreases rapidly as the pores are mostly filled and the internal surfaces are saturated. Within this subset of BET areas, the BETSI optimum is chosen as the one with the smallest percentage error under the 4th Rouquerol criterion, thus making the BET assignment unambiguous.

Next, we ran BETSI on the isotherms distributed in the round-robin experiment. In all cases, the spread of potential BETSI results (i.e., those in agreement with the Rouquerol criteria) was considerably narrower than that obtained by manual calculation (**Table 1**). **Figure 3**a shows the individual results from the social experiment and the comparison with the BETSI results; the corresponding variation coefficients are shown in Section S6 (Supporting Information) and an alternative representation normalized to the BETSI range is shown in Section S7 (Supporting Information). Since most groups reported using the Rouquerol criteria to calculate their BET areas, this substantiates our second hypothesis—that the manual implementation of the Rouquerol criteria is cumbersome and difficult to carry out in practice. For instance, in the case of NU-1104, the range of estimates decreases from 7500 $m^2\ g^{-1}$ in the social study to 235 $m^2\ g^{-1}$ under BETSI. Interestingly, some isotherms gave much larger spreads of results than others, suggesting that the BET model does not describe them as naturally and thus they are more susceptible to problems associated with the Rouquerol criteria. Unsurprisingly, we also observed this trend in the round-robin evaluation. To further investigate the goodness of the isotherm fittings, we define the BETSI variation

© 2022 The Authors. Advanced Materials published by Wiley-VCH GmbH

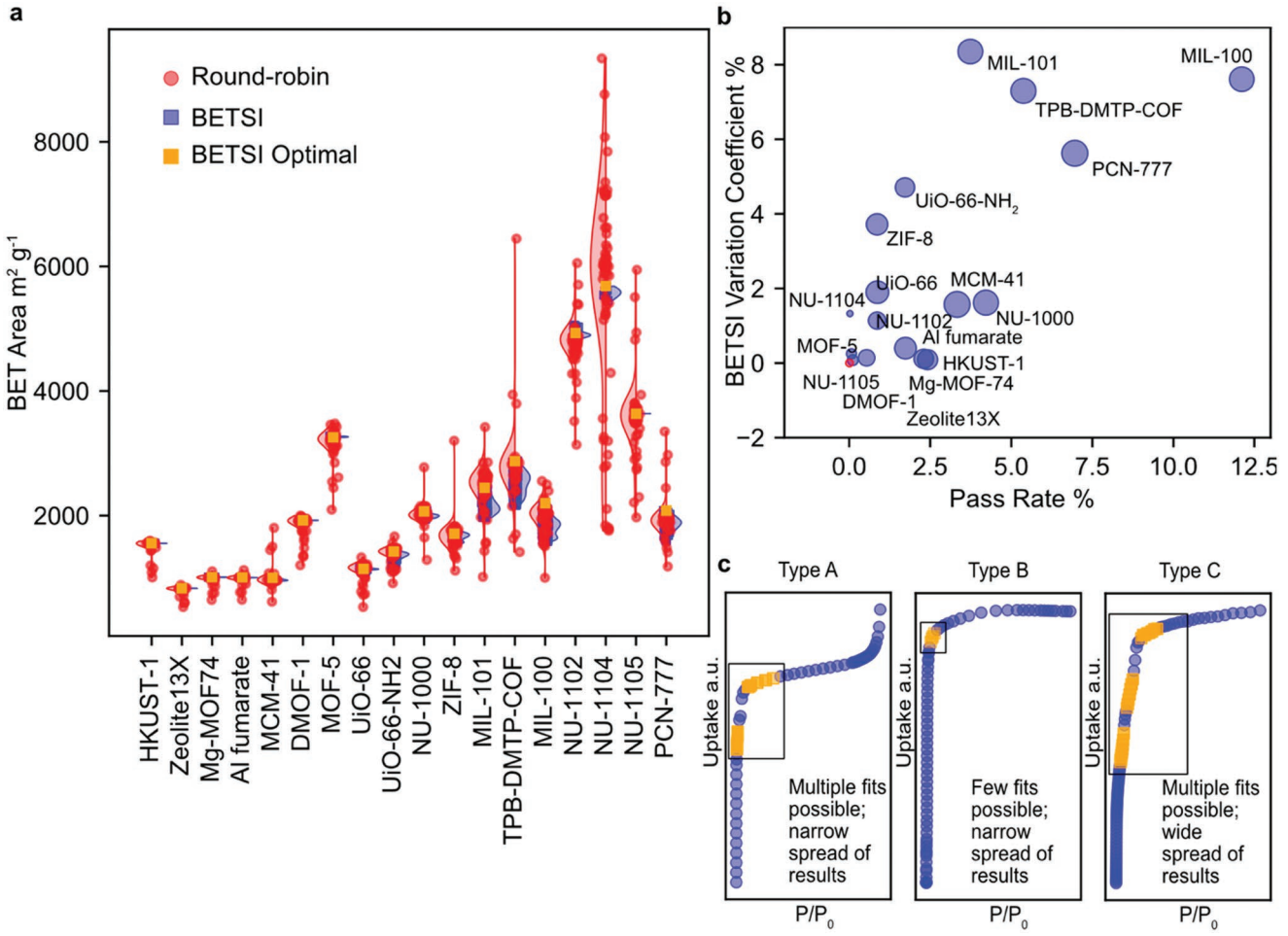


Figure 3. Social study results versus BETSI results. a) Distribution of BET areas for identical isotherms from the social study (red) and BETSI (blue) obtained by kernel density estimation (sample size for each material, $n = 61$). Superimposed is the BETSI optimum (yellow). Note that the distributions of values obtained by BETSI are considerably narrower in all cases than those in the social study. b) Plot of the BETSI variation coefficient (relative standard deviation of BETSI results) against the pass rate (fraction of valid fits against all hypothetical ones). Bubble size scales with the hit rate, the fraction of results from the social study that lie within the BETSI range. The red symbols have a hit rate of zero. Note the positive correlation between all three parameters. c) Isotherm fit classifications. Type A fits have a relatively wide fitting window, within which multiple fits are possible, but return a relatively narrow spread of BET results. Type B fits have a narrow fitting window and concomitantly return a narrow set of spread of results. Type C fits have wide fitting windows, which translates to multiple passable fits and a wide spread of permissible BET areas.

coefficient as the relative standard deviation of BETSI results, and the pass rate as the number of BET fits that pass under the Rouquerol criteria as a fraction of all potential fits. Further, the hit rate expresses the fractional number of BET areas calculated in the round-robin exercise that lie within the BETSI range. Figure 3b demonstrates the correlation between the pass rate, the BETSI variation coefficient, and the hit rate. Simply put, the more BET fits are valid, the greater the spread of possible BET areas is, and the more likely researchers are to satisfy the Rouquerol criteria in manual calculations. To account for the non-equal spacing of points on all different isotherms, the pressure-adjusted pass rate expresses the total sum of pressure intervals that fit Rouquerol criteria as a fraction of the sum of all pressure intervals of the hypothetical fitting ranges (Section S8, Supporting Information). From Figure 3b, we classify adsorption isotherms into three broad categories, types A, B, and C (Figure 3c). While it is difficult to generalize about the shape of these isotherms, we still offer some discussion of common features. Type A isotherms fit the BET model "best". Under BETSI, they have a relatively high pass rate and return a fairly narrow spread of results. Examples include materials such as Al-fumarate, NU-1000, Zeolite-13X, and MCM-41. Many of these isotherms do not have strongly pronounced isotherm knees and some have mesoporous steps. Hit rates greater than 70% are generally observed for these materials, suggesting that the majority of researchers did not struggle with the fittings. Type B isotherms only fit the BET model over a very limited range. These have extremely low pass rates, meaning that only few BET fits are valid, which in turn will be spread narrowly. Examples include MOF-5, DMOF-1, NU-1104, HKUST-1, and NU-1105. For the latter, out of 9409 hypothetical 10-point fits, only one is permissible under the Rouquerol criteria. Such prohibitively low pass rates make the correct BET assignment by hand virtually impossible and demonstrate the need for

© 2022 The Authors. Advanced Materials published by Wiley-VCH GmbH

computational support. In contrast to type A isotherms, type B isotherms often have sharp isotherm knees following strong adsorptive interactions at low relative pressures. Isotherms with more complex shapes such as NU-1104 also appear in this category. Type C isotherm fittings are arguably the most problematic. They have high pass rates and, concomitantly, they return large spreads of BET results. Typical materials that fit into this category are MIL-101, MIL-100, TPB-DMTP-COF and PCN-777. Like type A isotherms, these have rounded isotherm knees, which appear at higher relative pressures. It is for these materials that the necessity to extend the Rouquerol criteria is demonstrated and the BETSI algorithm makes an unambiguous BET assignment possible.

2. Outlook

BET theory is a great success story. Developed in the 1930s for non-microporous, open surfaces, it continues to this day to be applied to modern adsorbents with complex porosity. Despite the advances from classical density functional theory (DFT) methods, the BET area will likely continue playing a crucial role in porosimetry for decades to come, with impacts in energy research, transport, medical applications and climate-change mitigation. In light of these future developments, it will become increasingly important to share critical scientific metrics reliably to find a common language to report both academic and industrial progress.

Here, we have demonstrated the difficulties in unambiguously determining BET areas from adsorption isotherms, which, in turn, affect the assessment of material quality and reproducibility. These problems arise from imperfect and insufficient manual calculations and can only be met using modern computational methods. Furthermore, we propose BETSI as a step toward greater transparency and criticality in determining BET areas. We stress here that it is neither the function nor the purpose of BETSI to eliminate doubt and treat a particular BET area as "true." Researchers should remain aware of the limitations of BET theory when applied to microporous adsorbents in general and when BET areas are reported, the pressure range and number of points used should always be stated. We further recommend here that isotherms must be reported transparently and in detail, i.e., semi-log representation to show the low-pressure regions. The "experiment" is the adsorption isotherm—not the BET area.

3. Methods Section

3.1. Round-Robin Evaluation

N_2 adsorption isotherms of 18 different materials (Section S10, Supporting Information) were sent to international collaborators: HKUST-1, ZIF-8, NU-1000, MIL-101, UiO-66, Al fumarate, Zeolite13X, Mg-MOF-74, UiO-66-NH_2, MOF-5, DMOF-1, MCM-41, TPB-DMTP-COF, MIL-100, NU-1102, NU-1104, NU-1105, and PCN-777; they were anonymized and labelled A-R respectively. Note that this is not the order in which the isotherms appear in the paper. The isotherms were sampled from the A^2ML measurements and from the NIST Adsorption Database. Arbitrary scaling factors were introduced to minimize recollection bias of the isotherms. The isotherms were sent out in .csv format. All colleagues received the same email with the same set of instructions (Section S1, Supporting Information): to calculate the BET area from the data in the way they saw most fit and to report a rough estimate of how long it took them to calculate them. An anonymized one-page summary of each lab's own account of their calculation can be found in Section S11 (Supporting Information).

For easier data handling, once rescaled, all results were rounded to the next integer. None of the data points has been eliminated. The data is presented as a jitter plot for each material, with a superimposed kernel-density estimation obtained in Python.

3.2. BETSI

The BETSI algorithm, including executables (for Linux, Windows, and macOS) and a user manual are available at ref. [39]. The "How to Use BETSI" guide is included in the Supporting Infomation (Section S15). The program is written in Python and uses principally the NumPy library. It loops linear regressions over all consecutive combinations of at least three points, performs full BET analyses, and stores the fitting parameters in $n \times n$ results matrices, where the (j,i)-matrix element denotes a linear regression from the jth to the ith point on the isotherm. Binary pass/fail matrices with the same dimensionality are used independently to assess compliance with linearity and fitting criteria. The "filtering" of BET areas is achieved by element-wise matrix multiplication of the results matrices and the pass/fail matrices. This allows independent "activation" and "deactivation" of the criteria and observing the effects on the results. The minimum fitting requirement of ten points is coded in a pass/fail matrix to allow for some minimum point flexibility, as is the cut-off value for R^2 of 0.995. To avoid low-leverage non-linearity in the linear region, the first Rouquerol criterion has been extended to also require the linearized BET function to increase monotonically with P/P_0, as well as $N(1-(P/P_0))$. The third and fourth Rouquerol criteria are implemented through a 10 000-point Pchip interpolation of the isotherm to reconstruct the N_m (Read). As the third and fourth criteria require the N_m (BET) to be a real value, i.e., they require C to be positive, the second criterion cannot be independently deactivated from the third and the fourth. The associated logic has been written into the program. Following the BETSI filtering by multiplication of results and pass/fail matrices, the isotherm knee is identified as the subset of BET areas whose fitting region end on the highest permissible pressure point. In most cases, this will be the highest permissible point under the first Rouquerol criterion. The optimal BETSI prediction is chosen as the fitting region with the lowest percentage error under the fourth criterion and belonging to the isotherm knee subset.

BETSI only requires the adsorption isotherm as input data and returns six plots used to validate the results: the isotherm itself, with the optimal linear region highlighted as well as the BET fit; the "Rouquerol representation" of the isotherm, $N(1-(P/P_0))$ plotted against P/P_0; the linearized plot with the

© 2022 The Authors. Advanced Materials published by Wiley-VCH GmbH

OLS regression and the regression parameters; the filtered percentage error versus BET areas plot with the isotherm knee and optimal BET area highlighted; the filtered monolayer-loadings plot showing all permissible monolayer loadings on the isotherm; and the statistical distribution of permissible BET areas with a boxplot. Additionally, BETSI returns four regression diagnostics plots, which can be used to assess whether the assumptions of OLS regression have been met: the residuals versus fitted values plot can be used to visually inspect whether the residuals are normally distributed around the regression line, and similar information could be obtained from the QQ-plot. Finally, the scale-location plot can be used to assess whether the distribution of studentized residuals is homoscedatic or heteroscedatic and the residuals versus leverage plot can be used to identify high-leverage points that have an abnormally large influence on the regression line.

3.3. Comparison between Round-Robin Evaluation and BETSI Results

Statistical analysis of the results was performed in Python. The BETSI variation coefficient and the round-robin variation coefficient are standard deviations relative to the average of each set. The pass rate for each isotherm is the number of permissible BET fits as a fraction of all consecutive combination of points. To account for non-equal spacing of the points on each isotherm, the pressure-adjusted pass-rate is obtained by integrating along the pressure axis and dividing the total sum of permissive pressure intervals by the sum of all consecutive pressure intervals. The hit rate is the fractional number of BET areas calculated in the round-robin evaluation that lie within the BETSI range.

3.4. Statistical Analysis

Data was analyzed using the NumPy, SciPy, and Matplotlib libraries in Python. For the violin plots, a sample size, $n = 61$ was used for each material, and the estimator bandwidth for the kernel density estimator (KDE) was calculated using Scott's rule. For the bubble plots, the hit rate has been averaged over a sample size, $n = 61$, for each material.

Supporting Information

Supporting Information is available from the Wiley Online Library or from the author.

Acknowledgements

This project has received funding from the European Research Council (ERC) under the European Union's Horizon 2020 research and innovation programme (NanoMOFdeli), ERC-2016-COG 726380, Innovate UK (104384) and EPSRC IAA (IAA/RG85685). N.R. acknowledges the support of the Cambridge International Scholarship and the Trinity-Henry Barlow Scholarship (Honorary). O.K.F. and R.Q.S. acknowledge funding from the U.S. Department of Energy (DE-FG02-08ER15967). R.S.F. and D.B. acknowledge funding from the European Research Council (ERC) under the European Union's Horizon 2020 research and innovation programme (SCoTMOF), ERC-2015-StG 677289. Sandia National Laboratories is a multimission laboratory managed and operated by National Technology and Engineering Solutions of Sandia, LLC., a wholly owned subsidiary of Honeywell International, Inc., for the U.S. Department of Energy's National Nuclear Security Administration under contract DE-NA-0003525. The authors gratefully acknowledge funding from the U.S. Department of Energy, Office of Energy Efficiency and Renewable Energy, Hydrogen and Fuel Cell Technologies Office, through the Hydrogen Storage Materials Advanced Research Consortium (HyMARC). This paper describes objective technical results and analysis. Any subjective views or opinions that might be expressed in the paper do not necessarily represent the views of the U.S. Department of Energy or the United States Government. J.D.E. acknowledges the support of the Alexander von Humboldt Foundation and the Center for Information Services and High Performance Computing (ZIH) at TU Dresden. S.K.G. and S.M. acknowledge SERB (Project No. CRG/2019/000906), India for financial support. K.K. and R.K. acknowledge Active Co. Research Grant for funding. S.K. acknowledges funding from the European Research Council (ERC) under the European Union's Horizon 2020 research and innovation programme (COSMOS), ERC-2017-StG 756489. N.L. and J.G.M acknowledge funding from the European Commission through the H2020-MSCA-RISE-2019 program (ZEOBIOCHEM – 872102) and the Spanish MICINN and AEI/FEDER (RTI2018-099504-B-C21). N.L. thanks the University of Alicante for funding (UATALENTO17-05). ICN2 is supported by the Severo Ochoa program from the Spanish MINECO (Grant No. SEV-2017-0706) S.M.J.R. and A.L. wish to thank the Fund for Scientific Research Flanders (FWO), under grant nos. 12T3519N and 11D2220N. L.S. was supported by the EPSRC Cambridge NanoDTC EP/L015978/1. C.T.Y. and T.S.N. acknowledges funds from the National Research Foundation of Korea, NRF-2017M3A7B4042140 and NRF-2017M3A7B4042235. P.F. and H. Y. acknowledge US Department of Energy, Office of Basic Energy Sciences, Materials Sciences and Engineering Division under Award No. DE-SC0010596 (P.F.). R.O. would like to acknowledge funding support during his Ph.D. study from Indonesian Endowment Fund for Education-LPDP with the contract No. 202002220216006. Daniel Siderius: Official contribution of the National Institute of Standards and Technology (NIST), not subject to copyright in the United States of America. Daniel Siderius: Certain commercially available items may be identified in this paper. This identification does not imply recommendation by NIST, nor does it imply that it is the best available for the purposes described. B.V.L, S.T.E and A.M.P acknowledge funding from the European Research Council (ERC) under the European Union's Horizon 2020 Research and Innovation Program (Grant agreement no. 639233, COFLeaf).

Conflict of Interest

The authors declare no conflict of interest.

Author Contributions

J.W.M.O., J.R., D.M., and N.R. contributed equally to this work. J.W.M.O. and D.F-J. designed the study. J.W.M.O. and D.M. collected and curated the dataset of isotherms shared among co-authors. J.W.M.O., J.R., N.R., L.S. and B.C. developed BETSI code. All co-authors calculated the BET areas from the pre-measured isotherms. J.W.M.O., D.M., and D.F-J. co-wrote the paper. All authors discussed the results and contributed to the editing of the manuscript.

Keywords

adsorption, BET theory, porosimetry, porous materials, surface area

© 2022 The Authors. Advanced Materials published by Wiley-VCH GmbH

Received: February 15, 2022
Revised: March 21, 2022
Published online: May 23, 2022

[1] S. Brunauer, P. H. Emmett, E. Teller, *J. Am. Chem. Soc.* **1938**, *60*, 309.
[2] R. Cid, R. Arriagada, F. Orellana, *J. Catal.* **1983**, *80*, 228.
[3] D. Zhao, J. Feng, Q. Huo, N. Melosh, G. H. Fredrickson, B. F. Chmelka, G. D. Stucky, *Science* **1998**, *279*, 548.
[4] J. S. Beck, J. C. Vartuli, W. J. Roth, M. E. Leonowicz, C. T. Kresge, K. D. Schmitt, C. T. W. Chu, D. H. Olson, E. W. Sheppard, S. B. McCullen, J. B. Higgins, J. L. Schlenker, *J. Am. Chem. Soc.* **1992**, *114*, 10834.
[5] A. Corma, *Chem. Rev.* **1997**, *97*, 2373.
[6] S. Kitagawa, R. Kitaura, S. I. Noro, *Angew. Chem., Int. Ed.* **2004**, *43*, 2334.
[7] H. C. Zhou, J. R. Long, O. M. Yaghi, *Chem. Rev.* **2012**, *112*, 673.
[8] C. S. Diercks, O. M. Yaghi, *Science* **2017**, *355*, eaal1585.
[9] J. Li, J. Sculley, H. Zhou, *Chem. Rev.* **2012**, *112*, 869.
[10] O. K. Farha, A. Ö. Yazaydin, I. Eryazici, C. D. Malliakas, B. G. Hauser, M. G. Kanatzidis, S. T. Nguyen, R. Q. Snurr, J. T. Hupp, *Nat. Chem.* **2010**, *2*, 944.
[11] B. Li, H.-M. Wen, W. Zhou, B. Chen, *J. Phys. Chem. Lett.* **2014**, *5*, 3468.
[12] P. Z. Moghadam, T. Islamoglu, S. Goswami, J. Exley, M. Fantham, C. F. Kaminski, R. Q. Snurr, O. K. Farha, D. Fairen-Jimenez, *Nat. Commun.* **2018**, *9*, 1378.
[13] A. Corma, H. García, F. X. Llabrés i Xamena, *Chem. Rev.* **2010**, *110*, 4606.
[14] L. E. Kreno, K. Leong, O. K. Farha, M. Allendorf, R. P. Van Duyne, J. T. Hupp, *Chem. Rev.* **2012**, *112*, 1105.
[15] W. P. Lustig, S. Mukherjee, N. D. Rudd, A. V. Desai, J. Li, S. K. Ghosh, *Chem. Soc. Rev.* **2017**, *46*, 3242.
[16] P. Horcajada, R. Gref, T. Baati, P. K. Allan, G. Maurin, P. Couvreur, G. Férey, R. E. Morris, C. Serre, *Chem. Rev.* **2012**, *112*, 1232.
[17] I. Langmuir, *J. Am. Chem. Soc.* **1918**, *40*, 1361.
[18] Y. K. Tovbin, *Russ. Chem. Bull.* **1998**, *47*, 637.
[19] M. Thommes, K. Kaneko, A. V. Neimark, J. P. Olivier, F. Rodriguez-Reinoso, J. Rouquerol, K. S. W. Sing, *Pure Appl. Chem.* **2015**, *87*, 1051.
[20] K. S. W. Sing, D. H. Everett, R. A. W. Haul, L. Moscou, R. A. Pierotti, J. Rouquerol, T. Siemieniewska, *Pure Appl. Chem.* **1985**, *57*, 603.
[21] International Organization for Standardization (ISO), Ref. number ISO 2010, https://doi.org/10.1007/s11367-011-0297-3.
[22] J. Rouquerol, F. Rouquerol, P. Llewellyn, G. Maurin, K. S. W. Sing,*Adsorption by Powders and Porous Solids: Principles, Methodology and Applications*, 2nd ed., Elsevier, San Diego, CA, USA **2013**.
[23] F. Ambroz, T. J. Macdonald, V. Martis, I. P. Parkin, *Small Methods* **2018**, *2*, 1800173.
[24] D. A. Gómez-Gualdrón, P. Z. Moghadam, J. T. Hupp, O. K. Farha, R. Q. Snurr, *J. Am. Chem. Soc.* **2016**, *138*, 215.
[25] K. S. Walton, R. Q. Snurr, *J. Am. Chem. Soc.* **2007**, *129*, 8552.
[26] J. Park, J. D. Howe, D. S. Sholl, *Chem. Mater.* **2017**, *29*, 10487.
[27] P. Z. Moghadam, A. Li, S. B. Wiggin, A. Tao, A. G. P. Maloney, P. A. Wood, S. C. Ward, D. Fairen-Jimenez, *Chem. Mater.* **2017**, *29*, 2618.
[28] M. E. Davis, *Nature* **2002**, *417*, 813.
[29] H. Furukawa, K. E. Cordova, M. O'Keeffe, O. M. Yaghi, *Science* **2013**, *341*, 1230444.
[30] O. M. Yaghi, *J. Am. Chem. Soc.* **2016**, *138*, 15507.
[31] O. K. Farha, I. Eryazici, N. C. Jeong, B. G. Hauser, C. E. Wilmer, A. A. Sarjeant, R. Q. Snurr, S. T. Nguyen, A. Ö. Yazaydin, J. T. Hupp, *J. Am. Chem. Soc.* **2012**, *134*, 15016.
[32] T. C. Wang, W. Bury, D. A. Gómez-Gualdrón, N. A. Vermeulen, J. E. Mondloch, P. Deria, K. Zhang, P. Z. Moghadam, A. A. Sarjeant, R. Q. Snurr, J. F. Stoddart, J. T. Hupp, O. K. Farha, *J. Am. Chem. Soc.* **2015**, *137*, 3585.
[33] Z. Chen, P. Li, R. Anderson, X. Wang, X. Zhang, L. Robison, L. R. Redfern, S. Moribe, T. Islamoglu, D. A. Gómez-Gualdrón, T. Yildirim, J. F. Stoddart, O. K. Farha, *Science* **2020**, *368*, 297.
[34] I. M. Hönicke, I. Senkovska, V. Bon, I. A. Baburin, N. Bönisch, S. Raschke, J. D. Evans, S. Kaskel, *Angew. Chem., Int. Ed.* **2018**, *57*, 13780.
[35] D. Fairen-Jimenez, S. A. Moggach, M. T. Wharmby, P. A. Wright, S. Parsons, T. Düren, *J. Am. Chem. Soc.* **2011**, *133*, 8900.
[36] M. Agrawal, R. Han, D. Herath, D. S. Sholl, *Proc. Natl. Acad. Sci. USA* **2020**, *117*, 877.
[37] J. Rouquerol, P. Llewellyn, F. Rouquerol, *Stud. Surf. Sci. Catal.* **2007**, *160*, 49.
[38] *NIST/ARPA-E Database of Novel and Emerging Adsorbent Materials* (Eds: D.W. Siderius, V.K. Shen, R.D. JohnsonIII, R. d. vanZee), National Institute of Standards and Technology, Gaithersburg MD, USA, https://doi.org/10.18434/T43882 (accessed: August 2020).
[39] BET Surface Identification via Fairen Group at GitHub, https://github.com/fairen-group/betsi-gui (accessed: May 2022).

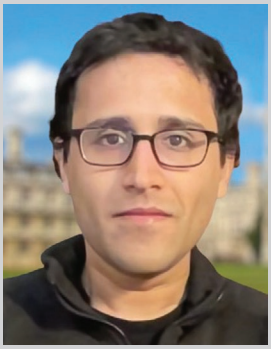


Johannes W. M. Osterrieth did his Ph.D. in the A^{2}ML Group under the supervision of Prof. David Fairen-Jimenez in the Department of Chemical Engineering and Biotechnology, University of Cambridge. He received his M.Chem. in chemistry at Oxford University (2016) and subsequently moved to Cambridge to join the EPSRC Doctoral Training Centre for Nanoscience and Nanotechnology (NanoDTC). His research interests lie in nanoparticle encapsulation into metal–organic frameworks and the fundamentals of adsorption models.

© 2022 The Authors. Advanced Materials published by Wiley-VCH GmbH



David Madden is currently a Marie Skłodowska-Curie Fellow at the University of Limerick, Ireland. He previously worked in the A^{2}ML Group as a Senior Research Associate under the mentorship of Prof. David Fairen- Jimenez in the Department of Chemical Engineering and Biotechnology, University of Cambridge. He completed his Ph.D. in physical chemistry in 2015 at the University of Limerick, and his research to date has focused on the use of novel porous materials for energy-efficient purifications, carbon capture and storage and inorganic materials scale-up while working with Prof. Michael Zaworotko, Prof. Gavin Walker, and Dr. Teresa Curtin at the Bernal Institute in the University of Limerick.



Nakul Rampal is currently a Ph.D. student in the A^{2}ML Group under the supervision of Prof. David Fairen-Jimenez. Prior to Cambridge, he completed his M.S. at the University of California, Berkeley where he was advised by Prof. Berend Smit. He did his undergraduate research at IIT Bombay, where he was advised by Prof. Ateeque Malani. He completed his undergraduate degree at Manipal Institute of Technology. His research deals with the development of novel algorithms using molecular simulation, high-performance computing, and machine learning, to accelerate the discovery of novel porous materials for applications such as carbon capture, energy storage, and drug delivery.



David Fairen-Jimenez is a professor of molecular engineering in the Department of Chemical Engineering & Biotechnology at the University of Cambridge, where he leads the Adsorption & Advanced Materials Laboratory (A^{2}ML). He got his Ph.D. in porous materials in chemistry from the University of Granada and worked later at the University of Edinburgh and Northwestern University. He leads an interdisciplinary lab that focuses on the study of adsorption in porous materials, combining advanced experimental techniques and computational modeling for energy and healthcare applications.

© 2022 The Authors. Advanced Materials published by Wiley-VCH GmbH